Spatial and Planar Optical Circuit (SPOC) Technology and Its Application to Photonic Network Devices

Yuzo Ishii, Yuichiro Ikuma, Kota Shikama, and Kenya Suzuki

Abstract

Because photonic networks have evolved from point-to-point systems to ring or mesh networks, higher scalability is required in the devices used in optical nodes. Hybridization of waveguide and free-space optics or spatial and planar optical circuits (SPOCs) may provide the necessary solutions to meet this requirement. A SPOC platform is attractive because it can take advantage of both waveguide technology and free-space optics. Waveguide technology provides a high degree of integration of optical functionality for such devices as splitters and non-wavelength selective switches, while free-space optics supplies a high degree of parallelism with two-dimensional spatial light modulators such as liquid crystal on silicon (LCOS) devices. In this article, we summarize the basics of SPOC technology and review its application to reconfigurable optical add/drop multiplexing (ROADM) devices. The key element of a waveguide on a SPOC platform is the spatial beam transformer, which has the same circuit structure as an arrayed waveguide grating but functions as a microlens array and provides attractive features such as dense integration of switches. An LCOS device has numerous phase modulating pixels, enabling flexible manipulation of lightwaves. We used a SPOC platform to construct and demonstrate several types of wavelength selective switches for ROADM applications.

Keywords: spatial and planar optical circuit (SPOC), wavelength selective switch, free-space optics

1. Introduction

As photonic networks have evolved from point-to-point systems to ring or mesh networks, reconfigurable optical add/drop multiplexing (ROADM) systems have been deployed, which are required to have colorless, directionless, and contentionless (CDC) capabilities [1]. Optical switching devices such as wavelength selective switches (WSSs) and multicast switches (MCSs) are important components in CDC-ROADM systems. Although waveguide-based WSSs were first proposed in early ROADM networks [2, 3], free-space optics based configurations have mainly been deployed in the actual systems only since the end of the last decade. The free-space optics based approach enables us to provide not only a sharp wavelength filter due to a high spatial resolution but also port scalability due to a high degree of parallelism. The MCS, on the other hand, is constructed based on waveguide technology [4] since it does not provide any wavelength-selective operation, which usually requires a bulk grating component located in the free space.

Combining waveguide technology with free-space optics can provide a solution that is not achievable using either method individually. The use of an arrayed waveguide grating (AWG) in combination with a MEMS (microelectromechanical systems)

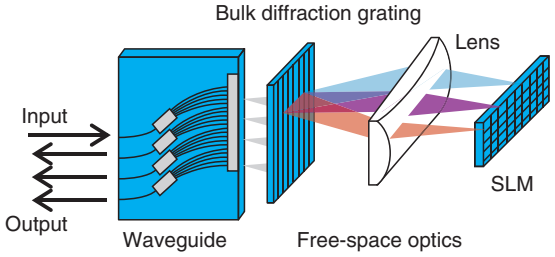

Fig. 1. SPOC concept; a waveguide device with highly controlled multiple beam emission is used as an I/O interface between fiber optics and free-space optics, and traditional bulk optics including a grating, lenses, and SLM are used in the latter part.

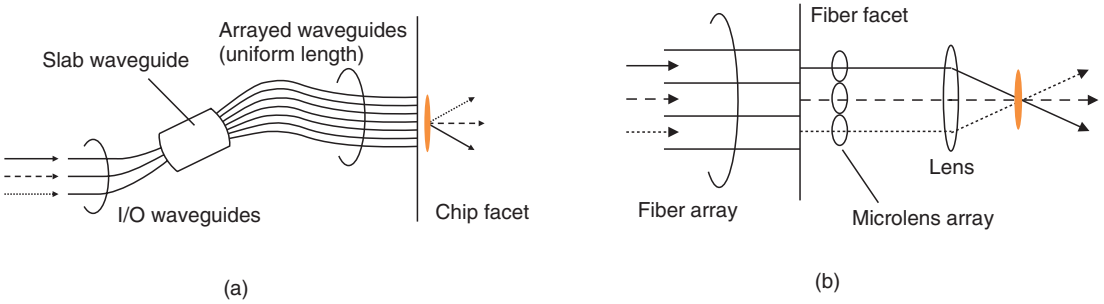

Fig. 2. Optical frontend configurations: (a) SBT circuit for launching three beams with different angles from the same position at the chip facet. (b) Equivalent optical design based on conventional discrete lenses.

mirror was first proposed in 2001 [5], and since then, several ideas including the use of a wavelength blocker [6, 7], tunable optical dispersion filter [8–13], and WSS [14–17] have been reported.

In this article, we describe our study, which is focused primarily on WSSs, and explain our concept of a spatial and planar optical circuit (SPOC) that combines the waveguide and free-space optics to get the best of both technologies.

2. SPOC [18]

An example of the SPOC concept is illustrated in **Fig. 1**. The waveguide frontend is used as an input/output (I/O) component for interfacing with the fiber optics and free-space optics, and traditional bulk optics including a grating, lenses, and spatial light modulator (SLM) are used in the free space to complete the design. The diffraction grating needed to implement the WSS is located with its dispersion axis aligned normal to the waveguide.

One unique and essential circuit element in the waveguide is a spatial beam transformer (SBT) [19], as shown in **Fig. 2(a)**. The SBT consists of multiple I/O waveguides, a slab waveguide, and arrayed waveguides. The SBT has a similar layout to that of a conventional AWG, but the path length difference of the arrayed waveguides is set to zero. It functions as follows. A lightwave input from the center input waveguide (indicated by the dashed arrow in Fig. 2(a)) spreads in the slab waveguide, couples to the arrayed waveguides, and exits from the chip facet to free space. Arrayed waveguides with a uniform path length difference maintain the wavefront of the lightwave so that a plane wave is output from the facet. Changing the input to another waveguide (indicated by a solid or dotted arrow) tilts the wavefront, so the output wavefront is also tilted.

Furthermore, it is also possible to bend the wavefront by controlling the path length among the arrayed waveguides so that one can launch not only a collimated beam but also a converging (or diverging) beam. The design flexibility in the SBT enables us to remove the discrete microlenses in the front of the fiber array. The equivalent optical design using conventional optics is shown in **Fig. 2(b)** for comparison.

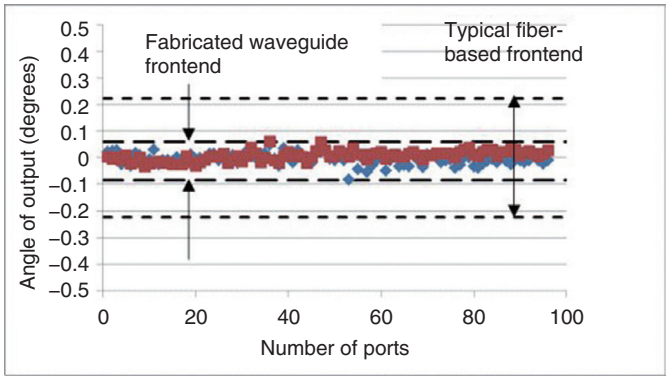

Fig. 3. Pointing accuracy measured for 96-SBT array. Red and blue dots respectively indicate TE (transverse-electric) and TM (transverse-magnetic) polarization.

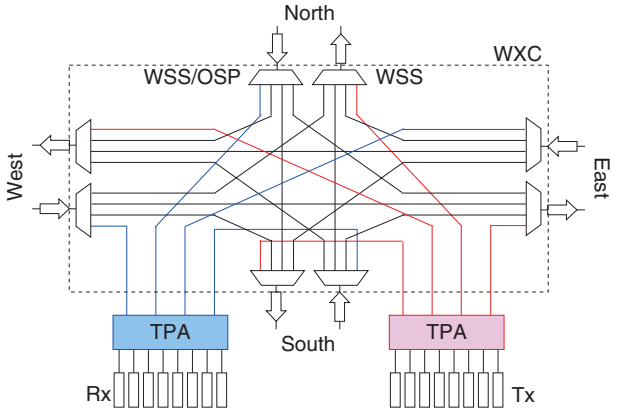

OSP: optical splitter
Rx: receiver
Tx: transmitter
WXC: wavelength cross-connect

Fig. 4. Schematic configuration of typical CDC-ROADM.

The integration of (micro)lenses means that the SBT is suitable for packaging the ports densely. Moreover, the beams are expected to be positioned well because there is no misalignment with the microlenses. The uniformity of the launched beam angle over 96 SBT circuits fabricated using the standard silica-based planar lightwave circuit (PLC) process is shown in **Fig. 3**. Excellent pointing accuracy less than +/-0.1 degrees was obtained for both polarizations, which is three times smaller than in the typical fiber-array-based frontend. The launch angle is translated into the transmission wavelength of a conventional AWG. Adjustment of the transmission wavelength in an AWG is well established, so the launch angle in the SBT can also be controlled well.

Some applications using SPOC are described in the following section.

3. Applications of SPOC

A typical node configuration for a CDC-ROADM network is shown in **Fig. 4**. The building blocks of each node consist of a WSS, a transponder aggregator (TPA), and optical amplifiers. Some of the wavelength division multiplexing (WDM) signals arriving at a node are routed by the WSS in different

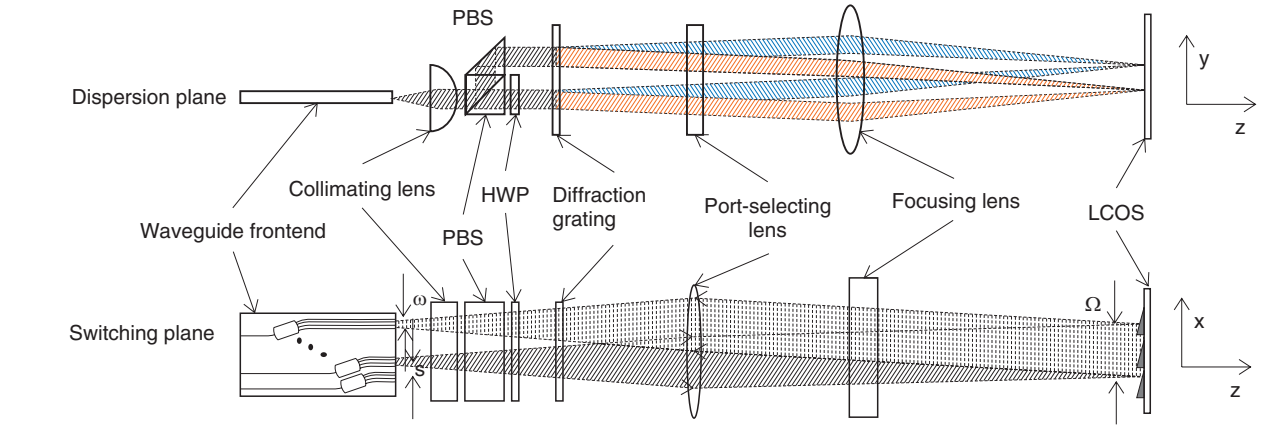

(a)

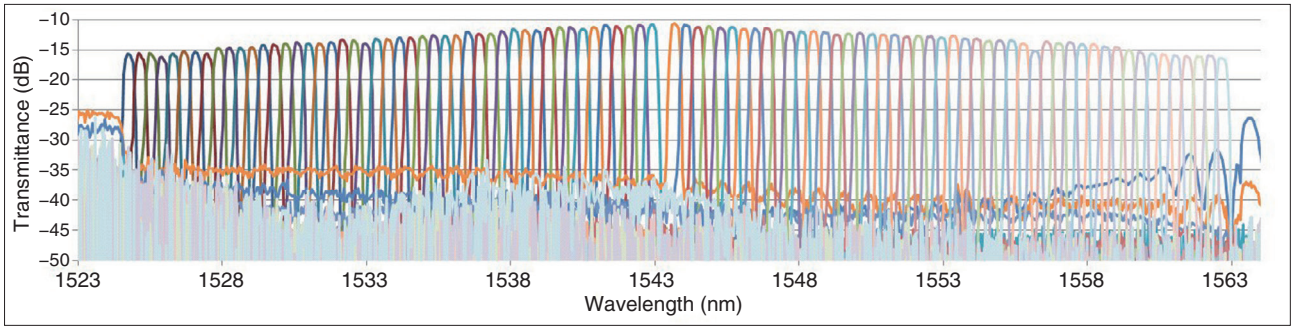

(b)

Fig. 5. (a) Optical system schematics of a 1 × 95 WSS in two orthogonal projections. (b) Superimposed transmission spectra of 95 curves that were taken at the different ports.

directions. The remaining signals are dropped and added at the node. They are directed from/to the TPA to/from the WSS.

3.1 Ultra-high port count WSS [20]

Port scalability is important for WSSs used in CDC-ROADM nodes because each node has to deal with a large number of WDM channels. For example, for an 8-degree node with 88 wavelength channels, the total number of WDM channels is 704. If 8 × 8 MCSs are used as the TPA, a WSS with 95 output ports (88 for the TPA; 7 for the other directions) is needed to achieve a drop rate of 100%.

The 1 × 95 WSS optical design using the SPOC technology is shown in **Fig. 5(a)**. This ultra-high port count WSS consists of a waveguide frontend, a collimating lens, polarization diversity optics (polarization beam splitter (PBS) and half-wave plate (HWP)), a diffraction grating, port-selecting and focusing cylindrical lenses, and an LCOS-based SLM.

The WDM signal input to the waveguide frontend is radiated into free space. The signal is collimated with a collimating lens in a direction normal to the waveguide substrate (y-axis). Because the LCOS is a polarization-sensitive device [21], we implemented polarization diversity optics in which the signal is split into two orthogonal linear polarizations along the y-axis. One of them is rotated 90 degrees with the HWP so that the linearly polarized signal is incident to the LCOS. The signal then passes through a diffraction grating of which the dispersion direction is along the y-axis. Next, the signal is collimated in the x-axis direction by the port-selecting lens and focused along the y-axis by the focusing lens. The SLM reflects the signal back along the same route to the frontend in the y-axis while it steers the signal so that

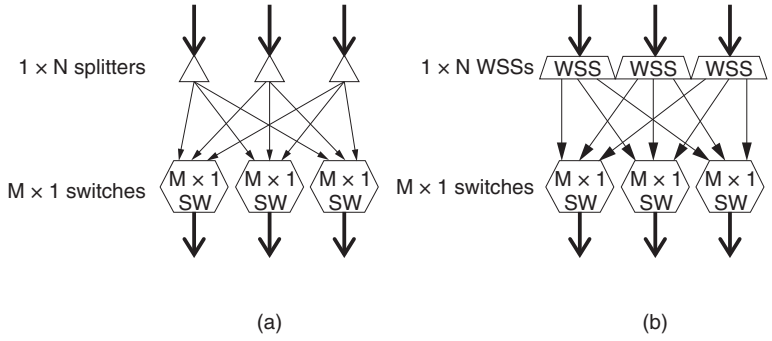

Fig. 6. Functional diagram of M × N TPAs: (a) MCS and (b) proposed low-loss TPA.

it hits a different position on the frontend in the x-axis. Hereafter, we call the x- and y-axes the switching and dispersion axis, respectively.

The SBT circuit was designed to have a beam radius of 26 μm at the chip facet with a port-to-port separation of 117 μm; therefore, the total effective aperture and physical chip size in the x-axis are only 11.2 and 17.5 mm, respectively. With the help of the high-dispersion grating, the respective focal lengths of the port-selecting and focusing lenses are 150 and 100 mm. The transmission spectra of the 1 × 95 WSS, in which each of the 95 WDM channels was routed to different output ports, is shown in **Fig. 5(b)**.

3.2 Low-loss TPA [22]

Another key device for constructing a CDC-ROADM node is a TPA; to date, a PLC-based MCS has been the only commercial solution. A block diagram of the MCS is shown in **Fig. 6(a)**. Incoming WDM signals are first broadcast by N, which is the number of transponders connected to the MCS. M units of the 1 × N splitters are integrated in one chip, where M is the number of degrees in the ROADM node. N units of M × 1 switches are also integrated to select one route of M degrees to send to a transponder.

Although the silica-based PLC has been matured and has proved to have high reliability, the MCS suffers from a principle loss of splitting. Therefore, it is becoming impractical with the scaling up in the number of transponders.

Another approach to implement the M × N TPA is shown in **Fig. 6(b)**. Here, M units of 1 × N WSSs and N units of M × 1 switches are connected. Unlike the MCS, each output port is connected to only one input port at a time; this is a necessary and sufficient functionality for a TPA because each transponder handles a single wavelength channel at a time. Since it has no splitters inside and therefore no intrinsic loss, this WSS-based TPA is preferable for a large scale TPA with large N compared to a conventional MCS-based TPA.

Using the SPOC platform enables the frontend of the M units of 1 × N WSSs and N units of 1 × M switches to be integrated in one chip, as shown in **Fig. 7(a)**. The M × 1 switch can be made with Mach-Zehnder interferometers in a tree arrangement with TO (thermo-optics) phase shifters, as shown in **Fig. 7(b)**. The diagram in Fig. 7(a) illustrates the case for M = 4 and N = 4. WDM signals from four different directions are input from the ports labeled *M fiber direction* and multiplexed in the angular domain by SBTs. They hit different areas on the LCOS, and each one supports a different WSS. This means that multiple WSSs can be angularly multiplexed.

The measured spectra of the fabricated 8 × 24 TPA are shown in **Fig. 8**, where 24 WDM signals of the 50-GHz-grid channel spacing in the C-band were independently routed to 24 output ports. The 24 graphs correspond to the output ports, and each plot has eight curves representing the input ports.

We can see directionless and contentionless switching from the set of graphs for output ports 1, 5, 9, and 13, where the same wavelengths from different input ports were routed to different output ports. Wavelength selective switching is clearly evident in the set of graphs for output ports 2, 6, 10, and 14, where four different channels from input port 3 were routed to different output ports. Flexible-grid operation is also clearly evident in the set of graphs for output ports 4, 8, 12, and 16, showing respectively that 50-, 100-, 150-, and 200-GHz transmission bands were obtained. The minimum insertion loss was 10.7 dB, which is lower than the theoretical loss of 13.8 dB of an MCS with the same port count.

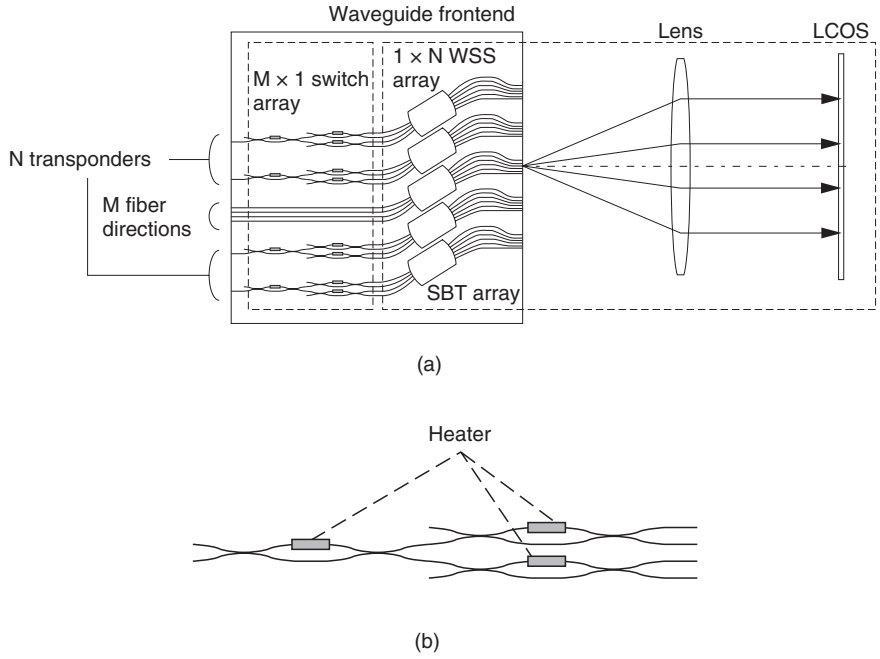

Fig. 7. (a) Optics schematic diagram of M × N TPA using SPOC and (b) schematic of non-wavelength selective M × 1 switch.

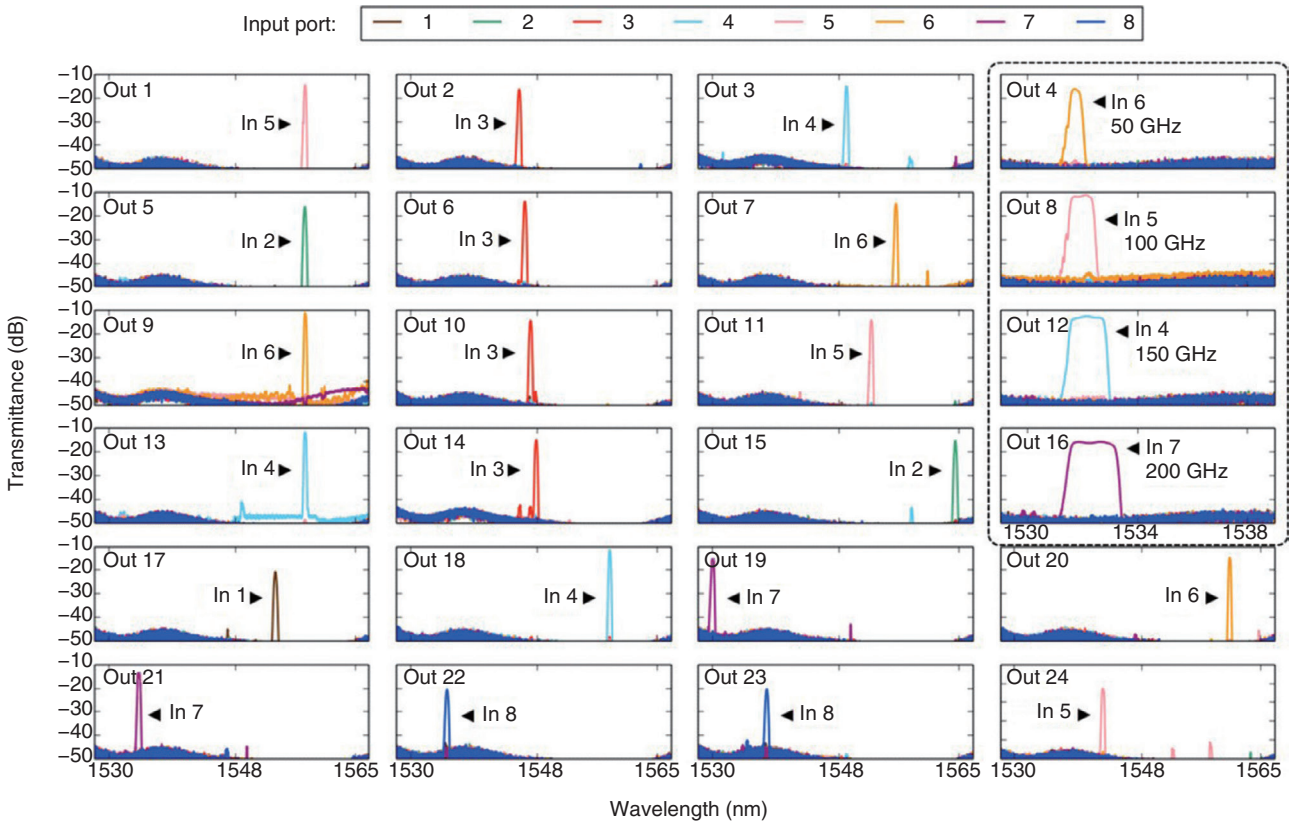

Fig. 8. Transmission spectra for 24 output ports of TPA (single polarization). A narrow wavelength range is shown for Out 4, 8, 12, and 16 to show the flexible-grid operation (dashed box).

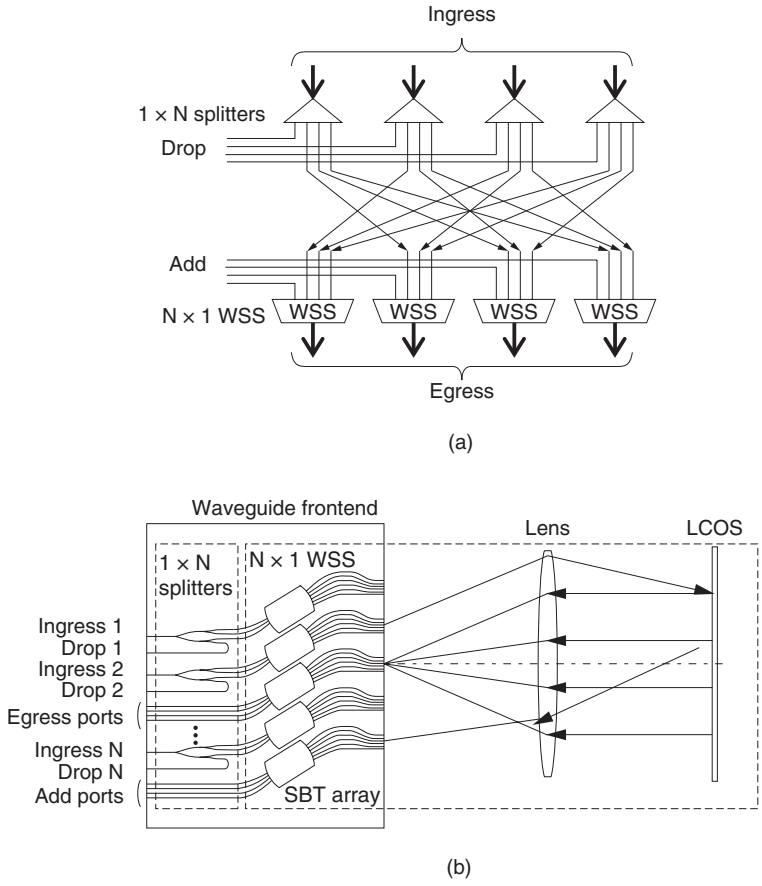

Fig. 9. N × N WXC: (a) functional diagram and (b) optics schematic diagram.

3.3 Integrated wavelength cross-connect with add/drop functionality

If we look again at Fig. 4, we can see many WSSs in the wavelength cross-connect (WXC) area, which is indicated by the dashed lines. WSS multiplexing is also useful for constructing a WXC.

Schematic diagrams of the functional block and optics system for the integrated WXC we constructed are shown in **Fig. 9** [23]. We used a broadcast-and-select type WXC configuration in which 1 × N splitters broadcast WDM signals from the ingress ports, and each N × 1 WSS selects one of them. The drop and add ports are used to access the TPAs. Because it is illogical to return a signal in the direction from which it originated, the splitter and the WSS for the same direction are not connected. The output ports of the splitters and the input ports of the WSSs that are not connected are used as drop and add ports. As shown in Fig. 9(b), N units of 1 × N splitters can be integrated into the waveguide frontend, and one of the split ports of each splitter is looped back to serve as a drop port. An SBT is integrated at the bottom of the waveguide frontend for use in adding ports.

The functionality of the constructed WXC was experimentally tested for channel bandwidths of 100, 150, and 200 GHz to evaluate the flexible-grid operation. Routing to Egress 5 as an example connection between the Ingress and Egress ports is shown in **Fig. 10(a)**. The plot shows that every input port was routed to every output port except for the ports with the same port number in each bandwidth. The connections for the Add and Egress ports are shown in **Fig. 10(b)**. Each Add port was routed to the corresponding Egress port without a splitter, so the insertion losses of the Add ports were lower than those of the Ingress ports. The losses from the Ingress to the Egress ports included an intrinsic splitting loss of 9 dB, which is inevitable due to the broadcast-and-select configuration.

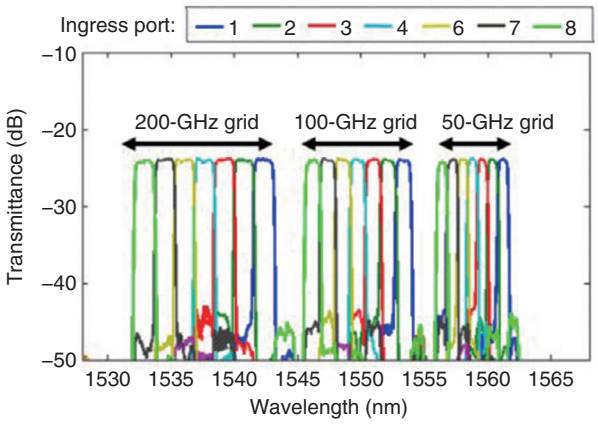

(a)

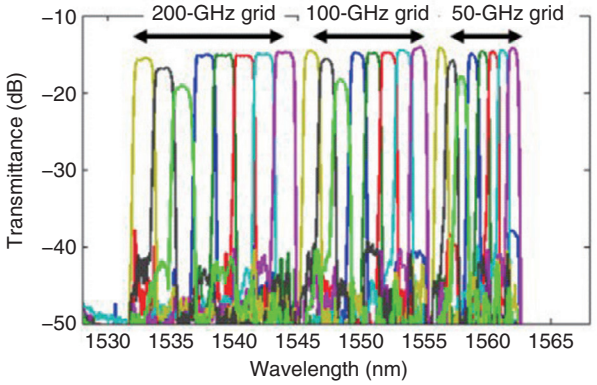

(b)

Fig. 10. Transmission spectra of 8 × 8 WXC: (a) all Ingress ports are configured to route to Egress port 5. (b) All Add ports are configured to route to the Egress port, where several-dB attenuations are provided to some ports. Better loss is seen due to the lack of 1 × 8 splitters (9-dB intrinsic loss).

4. Conclusion

We have described platform technology that combines two-dimensional planar waveguide photonics and three-dimensional free-space optics, which we call a spatial and planar optical circuit, or SPOC. The planar waveguide technology provides a high degree of integration of optical functionality for such devices as microlenses, splitters, and simple switches, while free-space optics supplies a high degree of parallelism with two-dimensional spatial light modulators such as LCOS devices.

With the unique advantages of SPOC, we demonstrated three applications for ROADM devices in a photonic network. These include the ultra-high port count 1 × 95 WSS, the low-loss 8 × 24 TPA, and the single module 8 × 8 WXC.

References

[1] Y. Sakamaki, T. Kawai, T. Komukai, M. Fukutoku, T. Kataoka, T. Watanabe, and Y. Ishii, "Experimental Demonstration of Multi-degree Colorless, Directionless, Contentionless ROADM for 127-Gbit/s PDM-QPSK Transmission System," Opt. Express, Vol. 19, No. 26, pp. B1–11, 2011.

[2] E. B. Basch, R. Egorov, S. Gringeri, and S. Elby, "Architectural Tradeoffs for Reconfigurable Dense Wavelength-division Multiplexing Systems," IEEE J. Sel. Topics Quant. Electron., Vol. 12, No. 4, pp. 615–626, 2006.

[3] T. Goh, T. Kitoh, M. Kohtoku, M. Ishii, T. Mizuno, and A. Kaneko, "Port Scalable PLC-based Wavelength Selective Switch with Low Extension Loss for Multi-degree ROADM/WXC," Proc. of the Optical Fiber Communication Conference and Exhibition/National Fiber Optic Engineers Conference (OFC/NFOEC) 2008, OWC6,

San Diego, CA, USA, Feb. 2008.
[4] T. Watanabe, K. Suzuki, and T. Takahashi, "Silica-based PLC Transponder Aggregators for Colorless, Directionless, and Contentionless ROADM," Proc. of OFC/NFOEC 2012, OTh3D.1, Los Angeles, CA, Mar. 2012.
[5] R. Ryf, P. Bernasconi, P. Kolodner, J. Kim, J. P. Hickey, D. Carr, F. Pardo, C. Bolle, R. Frahm, N. Basavanhally, C. Yoh, D. Ramsey, R. George, J. Kraus, C. Lichtenwalner, R. Papazian, J. Gates, H. R. Shea, A. Gasparyan, V. Muratov, J. E. Griffith, J. A. Prybyla, S. Goyal, C. D. White, M. T. Lin, R. Ruel, C. Nijander, S. Amey, D. T. Neilson, D. J. Bishop, S. Pau, C. Nuzman, A. Weis, B. Kumar, D. Lieuwen, V. Aksyuk, D. S. Greywall, T. C. Lee, H. T. Soh, W. M. Mansfield, S. Jin, W. Y. Lai, H. A. Huggins, D. L. Barr, R. A. Cirelli, G. R. Bogart, K. Teffeau, R. Vella, H. Mavoori, A. Ramirez, N. A. Ciampa, F. P. Klemens, M. D. Morris, T. Boone, J. Q. Liu, J. M. Rosamilia, and C. R. Giies, "Scalable Wavelength-selective Crossconnect Switch Based on MEMS and Planar Waveguides," Proc. of the 27th European Conference on Optical Communication (ECOC 2001), Th.F.4.11, Amsterdam, The Netherlands, Sept./Oct. 2001.
[6] N. Ooba, K. Suzuki, M. Ishii, A. Aratake, T. Shibata, and S. Mino, "Compact Wide-band Wavelength Blocker Utilizing Novel Hybrid AWG-free Space Focusing Optics," Proc. of OFC/NFOEC 2008, OWI2, San Diego, CA, USA, Feb. 2008.
[7] R. Rudnick, D. Sinefeld, O. Golani, and D. Marom, "One GHz Resolution Arrayed Waveguide Grating Filter with LCoS Phase Compensation," Proc. of OFC 2014, Th3F.7, San Francisco, CA, USA, Mar. 2014.
[8] K. Seno, K. Suzuki, K. Watanabe, N. Ooba, and S. Mino, "Channel-by-channel Tunable Optical Dispersion Compensator Consisting of Arrayed-waveguide Grating and Liquid Crystal on Silicon," Proc. of OFC 2008, OWP4, San Diego, CA, USA, Feb. 2008.
[9] K. Seno, K. Suzuki, N. Ooba, K. Watanabe, M. Ishii, H. Ono, and S. Mino, "Demonstration of Channelized Tunable Optical Dispersion Compensator Based on Arrayed Waveguide Grating and Liquid Crystal on Silicon," Opt. Express, Vol. 18, No. 18, pp. 18565–18579, 2010.
[10] K. Suzuki, N. Ooba, M. Ishii, K. Seno, T. Shibata, and S. Mino, "40-wavelength Channelized Tunable Optical Dispersion Compensator with Increased Bandwidth Consisting of Arrayed Waveguide Gratings and Liquid Crystal on Silicon," Proc. of OFC/NFOEC 2009, OThB3, San Diego, CA, USA, Mar. 2009.
[11] K. Seno, N. Ooba, K. Suzuki, T. Watanabe, M. Itoh, and T. Sakamoto, "Wide-passband 88-wavelength Channel-by-channel Tunable Optical Dispersion Compensator with 50-GHz Spacing," Proc. of OFC/NFOEC, 2011, OWM5, Los Angeles, CA, USA, Mar. 2011.
[12] D. Sinefeld and D. M. Marom, "Hybrid Guided-wave/Free-space Optics Photonic Spectral Processor Based on LCoS Phase Only Modulator," IEEE Photon. Technol. Lett., Vol. 22, No. 7, pp. 510–512, 2010.
[13] T. Tanaka, N. Ooba, M. Ishii, K. Seno, T. Watanabe, H. Ono, K. Suzuki, T. Sakamoto, and T. Takahashi, "Temperature Independent and Reduced Group Delay Ripple Operation of Multi-channel Tunable Optical Dispersion Compensator," Proc. of the Opto-Electronics and Communications Conference (OECC 2011), 7E2_4, Kaohsiung, Taiwan, July 2011.
[14] T. Ducellier, A. Hnatiw, M. Mala, S. Shaw, A. Mank, D. Touahri, D. McMullin, T. Zahmi, B. Lavigne, P. Peloso, and O. Leclerc, "Novel High Performance Hybrid Waveguide-MEMS 1x9 Wavelength Selective Switch in a 32-Cascade Loop Experiment," Proc. of ECOC 2001, Th.F.4.11(PD), Amsterdam, The Netherlands, Sept./Oct. 2001.
[15] S. Yuan, N. Madamopoulos, R. Helkey, V. Kaman, J. Klingshirn, and J. Bowers, "Fully Integrated NxN MEMS Wavelength Selective Switch with 100% Colorless Add-Drop Ports," Proc. of OFC/NFOEC, 2008, OWC2, San Diego, CA, USA, Feb. 2008.
[16] K. Sorimoto, H. Tsuda, H. Ishikawa, T. Hasama, H. Kawashima, K. Kintaka, M. Mori, and H. Uetsuka, "Polarization Insensitive Wavelength Selective Switch Using LCOSs and Monolithically Integrated Multi-layered AWG," Proc. of OECC 2010, 6E2-4, Sapporo, Japan, July 2010.
[17] D. M. Marom, C. R. Doerr, M. A. Cappuzzo, E. Y. Chen, A. Wong-Foy, L. T. Gomez, and S. Chandrasekhar, "Compact Colorless Tunable Dispersion Compensator with 1000-ps/nm Tuning Range for 40-Gb/s Data Rates," IEEE J. Lightwave Technol., Vol. 24, No. 1, pp. 237–241, 2006.
[18] K. Suzuki and Y. Ikuma, "Spatial and Planar Optical Circuit," Proc. of OFC 2016, Th3E.1, Anaheim, CA, USA, Mar. 2016.
[19] K. Seno, K. Suzuki, N. Ooba, T. Watanabe, M. Itoh, T. Sakamoto, and T. Takahashi, "Spatial Beam Transformer for Wavelength Selective Switch Consisting of Silica-based Planar Lightwave Circuit," Proc. of OFC/NFOEC 2012, JTh2A.5, Los Angeles, CA, USA, Mar. 2012.
[20] K. Suzuki, Y. Ikuma, E. Hashimoto, K. Yamaguchi, M. Itoh, and T. Takahashi, "Ultra-high Port Count Wavelength Selective Switch Employing Waveguide-based I/O Frontend," Proc. of OFC 2015, Tu3A.7, Los Angeles, CA, USA, Mar. 2015.
[21] See, for example, K. M. Johnson, D. J. McKnight, and I. Underwood, "Smart Spatial Light Modulators Using Liquid Crystals on Silicon," IEEE J. Quantum Electron., Vol. 29, No. 2, pp. 699–714, 1993.
[22] Y. Ikuma, K. Suzuki, N. Nemoto, E. Hashimoto, O. Moriwaki, and T. Takahashi, "Low-loss Transponder Aggregator Using Spatial and Planar Optical Circuit," IEEE J. Lightwave Technol., Vol. 34, No. 1, pp. 67–72, 2016.
[23] N. Nemoto, Y. Ikuma, K. Suzuki, O. Moriwaki, T. Watanabe, M. Itoh, and T. Takahashi, "8 x 8 Wavelength Cross Connect with Add/Drop Ports Integrated in Spatial and Planar Optical Circuit," Proc. of ECOC 2015, Tu.3.5.1, Valencia, Spain, Sept./Oct. 2015.

Yuzo Ishii
Senior Research Engineer, Supervisor, Product Strategy Planning Project, NTT Device Innovation Center.

He received his B.S., M.S., and Ph.D. in precision machinery engineering from the University of Tokyo in 1995, 1997, and 2005. In 1997, he joined NTT Optoelectronics Laboratories, where he engaged in research on microoptics for chip-to-chip optical interconnection. During 2005–2006, he was a visiting researcher at Vrije University in Brussels, Belgium. From 2013 to 2014, he was with NTT Electronics Corporation, where he worked on the development and commercialization of WSSs. He is a member of the Japan Society of Applied Physics.

Yuichiro Ikuma
Researcher, Optical Transmission Systems Development Project, Transport Network Innovation Project, NTT Network Service Systems Laboratories.

He received his B.E., M.E., and Ph.D. in electronics and electrical engineering from Keio University, Kanagawa, in 2007, 2009, and 2012. From 2009 to 2012, he was a research fellow of the Japan Society for the Promotion of Science. Since joining NTT Photonics Laboratories in 2012, he has been involved in the development of optical switches for ROADM systems. He is currently with NTT Network Service Systems Laboratories. He is a member of the Institute of Electrical and Electronics Engineers (IEEE) Photonics Society and the Institute of Electronics, Information and Communication Engineers (IEICE).

Kota Shikama
Researcher, Optoelectronic Subsystem Research Group, Photonics-Electronics Convergence Laboratory, NTT Device Technology Laboratories.

He received a B.E. and M.E. in materials science from Keio University, Kanagawa, in 2008 and 2010. In 2010, he joined NTT Photonics Laboratories. He has been conducting research on optical connectors, optical packaging technologies, and optical node modules. He received the Young Award from IEEE CPMT (Components, Packaging and Manufacturing Technology) Symposium Japan in 2012 and the Young Engineer Award from IEICE in 2014. He is a member of IEICE and IEEE.

Kenya Suzuki
Senior Research Engineer, Supervisor, Optoelectronics Integration Research Group, Photonics-Electronics Convergence Laboratory, NTT Device Technology Laboratories.

He received a B.E. and M.E. in electrical engineering and a Dr. Eng. in electronic engineering from the University of Tokyo in 1995, 1997, and 2000. He joined NTT in 2000. From September 2004 to September 2005, he was a visiting scientist at the Research Laboratory of Electronics (RLE) at the Massachusetts Institute of Technology, USA. From 2008 to 2010, he was with NTT Electronics Corporation, where he worked on the development and commercialization of silica-based waveguide devices. He has also been a guest chair professor at the Tokyo Institute of Technology since 2014. His research interests include optical circuit design and optical signal processing. He received the Young Engineer Award from IEICE in 2003. He is a member of IEICE, IEEE, and the Physical Society of Japan.